Chapter 11
Separable Potentials Model for Atoms and Molecules in Strong Ultrashort Laser Pulses

Yu. V. Popov, A. Galstyan, B. Piraux, P. F. O'Mahony, F. Mota-Furtado, P. Decleva and O. Chuluunbaatar

Abstract In this contribution, we discuss a model based on the replacement of the potential describing the interaction of a single active electron with the nucleus or the nuclei of atoms or molecules, with a potential, separable in momentum space and consisting of several terms. Each term supports only one single electron bound state of the system. We apply this model to the description of the interaction of atomic and molecular hydrogen, hydrogen anion and water molecule with an external ultrashort laser pulse. As expected, this short range separable potential model works very well for the hydrogen negative ion due to the short range nature of it real potential. In the case of other systems, we show that, at high frequency, taking into account the

Yu. V. Popov
Skobeltsyn Institute of Nuclear Physics, Lomonosov Moscow State University, Moscow, Russia
e-mail: popov@srd.sinp.msu.ru

Yu. V. Popov · O. Chuluunbaatar
Joint Institute for Nuclear Research, Dubna, Moscow 141980, Russia
e-mail: chuka@jinr.ru

A. Galstyan (✉) · B. Piraux
Institute of Condensed Matter and Nanosciences, Université Catholique de Louvain, 2 Chemin du Cyclotron, L7.01.07, 1348 Louvain-la-Neuve, Belgium
e-mail: alexander.galstyan@uclouvain.be

B. Piraux
e-mail: bernard.piraux@uclouvain.be

P. F. O'Mahony · F. Mota-Furtado
Department of Mathematics, Royal Holloway, University of London, Egham, Surrey TW20 0EX, UK
e-mail: p.omahony@rhul.ac.uk

F. Mota-Furtado
e-mail: f.motafurtado@rhul.ac.uk

P. Decleva
Dipartimento di Scienze Chimiche e Farmaceutiche, Universita' di Trieste, Trieste, Italy
e-mail: decleva@units.it

O. Chuluunbaatar
Institute of Mathematics, National University of Mongolia, UlaanBaatar, Mongolia

K. Yamanouchi et al. (eds.), *Progress in Photon Science*, Springer Series in Chemical Physics 119, https://doi.org/10.1007/978-3-030-05974-3_11

long range interaction in the final state is equivalent to multiplying the ionisation probability by a constant factor independent of the laser parameters.

11.1 Introduction

Nonlocal two-particle separable potentials are widely used in nuclear physics. For more than two particle scattering processes, they might significantly simplify the calculation of matrix elements, in particular if it involves the evaluation of the two-body scattering amplitudes (see e.g. [1]). In some cases, one can even solve the problem analytically, e. g. when a light particle interacts with two heavy ones (see Takibayev [2]). This model was applied to study the structure of H_2^+ by the same author, but to our regret this paper exists only in Russian and does not have an online version [3]. It is important to note at this stage that in the configuration space the separable potential has a short range.

Given the simplicity of the calculations, the separable potentials can be applied to treat the laser-matter interactions. In this case, the main difficulty is the long range of the Coulomb interaction, which is usually dominating. Besides this problem, the use of separable potentials raises additional questions:

- Can a separable potential be uniquely defined?
- The observables in the presence of the electromagnetic field should be gauge invariant. In quantum physics the gauge invariance is assured by a property of locality of the potentials. What to do with separable non-local potentials?
- What is the predictive power of this model? Does it allow to find new mechanisms and processes in the domain of its validity?

These are the questions we are trying to answer in this chapter.

The model we consider here (we abbreviate it below by SPAM for Separable Potentials for Atoms and Molecules), was first introduced in [4] to describe the interaction of atomic hydrogen with a laser pulse. The separable potentials are defined in terms of the bound state wave functions, and the continuum functions are obtained by solving the stationary Schrödinger equation. Subsequently in [5–8], more complicated potentials have been considered and the calculation of different observables in the case of atomic hydrogen interacting with a laser pulse has been discussed in detail.

Electron energy and angular spectra in the case of atomic hydrogen, interacting with an external electromagnetic field of fixed frequency, have been measured [9–16]. On the other hand, a robust numerical code exists that is solving the time dependent Schrödinger equation (TDSE) by decomposing the initial wave function in a Sturmian basis and propagating it during its interaction with a laser pulse [17, 18]. Thus it is possible to compare our SPAM results to both experimental data and results of "exact" numerical calculations, such as TDSE based simulations, which may be considered as "numerical experiments". Finally, separable potentials have been also used in [19, 20], focusing, in particular, on the gauge invariance problem.

It is worth noting that the SPAM model is related to the strong field approximation (SFA) [21]. We remind here that SFA neglects the Coulomb potential after the emission of the electron when the electric field is sufficiently intense. In this case, the solution of the TDSE with a time dependent dipole interaction potential is a Volkov wave, so that the transition matrix elements in the length gauge and in the velocity gauge can be easily calculated. We can generalise it and build an iterative series in the Coulomb potential, which allows one to calculate the SFA wave packet at different orders in the Coulomb potential [22]. This approximation has, however, serious drawbacks:

- it is gauge dependent;
- the series has been shown to diverge in some situations [23].

Finally, within the single active electron (SAE) approximation, the SPAM can be applied to many-electron systems. The SAE approximation is used in the case of a single electron ionisation of a complex target by different projectiles, in particular by a laser pulse. The main idea behind the SAE approximation is that only one electron in the atomic (molecular) target is interacting with the projectile, and this is the electron which leaves the target. All other electrons are frozen. This model is working pretty well in the case of high energy projectiles, when the momentum of the ejected particle is much higher than a characteristic velocity of the target electrons, meaning that the transferred momentum has to be big. Conversely, if it is not the case, then the slow electron inelastically interacts with other electrons, and the SAE model is no longer applicable. For example, if the core electron is ejected from the atom, this vacancy will be filled with outer electrons, which could lead to cascade processes and, possibly, auto-ionisation. The SAE model would work well only if the ejection of the electron is much faster than these subsequent processes. We therefore expect that the SAE model can be successfully applied for the outer orbital ionisation.

All these features will be discussed in more detail below. Atomic units (a.u.), in which $\hbar = e = m_e = 1$, are used throughout unless otherwise specified.

11.2 Atomic Hydrogen

11.2.1 Preliminary Remarks on Gauge Invariance

The property of gauge invariance of theories which include the electromagnetic field is a central problem of such theories. This property allows one to obtain various equivalent forms of the Schrödinger equation related to each other through unitary transformations: this leads to the invariance of the physical observables. Let us recall that the Maxwell equations can be written in terms of the scalar and vector potentials, $U(\mathbf{r}, t)$ and $\mathbf{A}(\mathbf{r}, t)$. These potentials determine unambiguously the electric and magnetic fields. However, the potentials themselves are not uniquely defined. For

example, two sets of potentials $(\mathbf{A}', U')$ and $(\mathbf{A}, U)$, where

$$\mathbf{A}' = \mathbf{A} + \nabla f, \qquad U' = U - \frac{1}{c}\frac{\partial f}{\partial t},$$

give the same electric and magnetic fields for an arbitrary scalar function $f(\mathbf{r}, t)$.

The electric field $\mathbf{E}$ is related to the potentials as follows:

$$\mathbf{E}(\mathbf{r}, t) = -\frac{1}{c}\frac{\partial}{\partial t}\mathbf{A}(\mathbf{r}, t) - \nabla U(\mathbf{r}, t). \tag{11.1}$$

In the so-called Coulomb gauge it is assumed that

$$\mathrm{div}\mathbf{A} = 0.$$

Furthermore, one makes a physical assumption about weak dependence of the scalar potential on the coordinate within the atom, i.e.

$$U(\mathbf{r}, t) \simeq U(0, t),$$

which allows one to neglect the gradient of the scalar potential in (11.1). In addition, we write

$$\mathbf{A}(\mathbf{r}, t) \simeq \mathbf{A}(0, t) = \mathbf{A}(t).$$

which is the well known dipole approximation.

In the following, we consider a linearly polarised pulsed field which means that the vector potential can be written as $\mathbf{A}(t) = \mathbf{e}A(t)$, where $\mathbf{e}$ is the unit polarisation vector[1] and

$$A(t) = \sqrt{\frac{I}{I_0}}\sin^2\left(\pi\frac{t}{T}\right)\sin(\omega t), \quad 0 \le t \le T.$$

Here ω is field frequency, $T = \frac{2\pi N}{\omega}$ is the total pulse duration where N is the number of optical cycles and I is the peak intensity of the pulse with $I_0 = 3.5 \times 10^{16}$ W/cm^2. It is important to note that $A(t)$ must be zero before and after the laser pulse.

Consider the TDSE in velocity form (V-form) describing the interaction between an electric pulse and a hydrogen-like atom which is initially in its ground state,

$$\left[\mathrm{i}\frac{\partial}{\partial t} - \frac{1}{2}\left(-\mathrm{i}\nabla + \frac{1}{c}\,\mathbf{e}A(t)\right)^2 + \frac{Z}{r}\right]\Phi_V(\mathbf{r}, t) = 0, \quad \Phi_V(\mathbf{r}, 0) = \varphi_0(r) = \sqrt{\frac{Z^3}{\pi}}e^{-Zr},$$

$$\int \mathrm{d}^3 r|\Phi_V(\mathbf{r}, t)|^2 = 1, \tag{11.2}$$

[1]The approach is not limited to linear polarisation of the external field or a particular form of the envelope.

where Z designates the nuclear charge. By using the well known unitary Göppert-Mayer transformation that relates the full wave packet in velocity and length gauges,

$$\Phi_V(\mathbf{r},t) = \exp\left[-\mathrm{i}\frac{1}{c}A(t)(\mathbf{er})\right]\Phi_L(\mathbf{r},t), \tag{11.3}$$

we obtain from (11.2) the length form (L-form) of the TDSE:

$$\left[\mathrm{i}\frac{\partial}{\partial t} + \frac{1}{2}\triangle - E(t)(\mathbf{er}) + \frac{Z}{r}\right]\Phi_L(\mathbf{r},t) = 0, \quad \Phi_L(\mathbf{r},0) = \varphi_0(r).$$

Here $E(t) = -\frac{1}{c}\frac{\partial A(t)}{\partial t}$.

Usually one requires a good numerical algorithm to obtain a good agreement of the computed observables (level populations, electron angular and energy distributions etc.) in the L- and V- forms. In the exact theory they must be identical. In the momentum space the V-form TDSE takes the form

$$\left[\mathrm{i}\frac{\partial}{\partial t} - \frac{1}{2}(\mathbf{p} + \frac{1}{c}A(t)\mathbf{e})^2\right]\tilde{\Phi}_V(\mathbf{p},t) + \int \frac{\mathrm{d}^3u}{(2\pi)^3}\frac{4\pi Z}{|\mathbf{p}-\mathbf{u}|^2}\tilde{\Phi}_V(\mathbf{u},t) = 0, \tag{11.4}$$

$$\tilde{\Phi}_V(\mathbf{p},0) = \tilde{\varphi}_0(p) = \frac{8\sqrt{\pi Z^5}}{(p^2+Z^2)^2}.$$

In (11.4), the function $\tilde{\Phi}_V(\mathbf{p},t)$ designates the Fourier transform of the function $\Phi_V(\mathbf{r},t)$. Similarly, the L-form TDSE becomes

$$\left[\mathrm{i}\frac{\partial}{\partial t} - \frac{p^2}{2} - \mathrm{i}E(t)(\mathbf{e}\cdot\nabla_p)\right]\tilde{\Phi}_L(\mathbf{p},t) + \int \frac{\mathrm{d}^3u}{(2\pi)^3}\frac{4\pi Z}{|\mathbf{p}-\mathbf{u}|^2}\tilde{\Phi}_L(\mathbf{u},t) = 0,$$

$$\tilde{\Phi}_L(\mathbf{p},0) = \tilde{\varphi}_0(p), \tag{11.5}$$

and the gauge transformation (11.3) becomes

$$\tilde{\Phi}_V(\mathbf{p},t) = \tilde{\Phi}_L(\mathbf{p} + \frac{1}{c}A(t)\mathbf{e},t).$$

Equations (11.4) and (11.5) are the basic ones that we use in our SPAM model.

11.2.2 Definition of Separable Potentials

First of all and based on [24, 25], it is possible to show that the kernel of the Coulomb potential may be expanded as follows

$$\frac{4\pi Z}{|\mathbf{p}-\mathbf{u}|^2} = \frac{(2\pi)^2 Z}{pu}\sum_{l=0}^{\infty}(l!)^2\left(\frac{4qp}{q^2+p^2}\right)^{l+1}\left(\frac{4qu}{q^2+u^2}\right)^{l+1}\times$$

$$\sum_{m=-l}^{l} Y^*_{l,m}(\theta_p,\phi_p)Y_{l,m}(\theta_u,\phi_u)\sum_{n=0}^{\infty}\frac{n!}{(n+2l+1)!}C_n^{l+1}\left[\frac{q^2-p^2}{q^2+p^2}\right]C_n^{l+1}\left[\frac{q^2-u^2}{q^2+u^2}\right]. \tag{11.6}$$

In other words, this Coulomb kernel may be expanded as a sum of products of separable potentials, given by Gegenbauer polynomials $C_n^{l+1}(x)$. Note that this expansion is not unique since it depends on the arbitrary parameter q. In practice, we have to truncate the infinite expansion. In this case we deal again with a sum of the short range separable potentials, and q determines their range in the configuration space [8]. Equation (11.6) presents one way to define non-local separable potentials. Here, however, we focus on a different method.

Before describing this method in more detail, let us discuss a few important points. The approximation of a singular local potential by a non-singular non-local potential raises some questions about the validity of this approximation. Instead of the long range Coulomb potential that gives rise to an infinite number of bound states, we obtain a short range potential with a finite number of bound states. In fact, this problem exists only in theory, as in the reality the potential is always truncated. Moreover, the locality of the potential is an approximation as well. Finally, the gauge invariance is a feature of a theory with a local potential only. Separable potential theories cannot be gauge invariant. However, as we see below, separable potentials are very useful for calculations, and they allow one to investigate the dominating mechanisms. In the second method, we approximate the Coulomb potential in the following way

$$\frac{4\pi Z}{|\mathbf{p}-\mathbf{u}|^2} \approx \sum_{n=0}^{N}\sum_{l=0}^{L}\sum_{m=-l}^{l} v_{nl}(p)Y_{l,m}(\theta_p,\phi_p)\, v^*_{nl}(u)Y^*_{l,m}(\theta_u,\phi_u).$$

The components $v_{nl}(p)$ of the separable potential correspond to some eigenfunctions of the Hamiltonian with the Coulomb potential

$$\left(\varepsilon_j - \frac{p^2}{2}\right)\tilde{\varphi}_j(\mathbf{p}) + \sum_{q=1}^{N}\sum_{l=0}^{L}\sum_{m=-l}^{l} v_{ql}(p)Y_{l,m}(\theta_p,\phi_p)\times \left[\int \frac{\mathrm{d}^3u}{(2\pi)^3}v^*_{ql}(u)Y^*_{l,m}(\theta_u,\phi_u)\tilde{\varphi}_j(\mathbf{u})\right] = 0, \tag{11.7}$$

where $\tilde{\varphi}_j(\mathbf{p}) = \tilde{\varphi}_{jl_j}(p)Y_{l_j,m_j}(\theta_p,\phi_p)$ are the Coulomb bound state eigenfunctions. By substituting in (11.7), we get

$$\left(\varepsilon_j - \frac{p^2}{2}\right)\tilde{\varphi}_{jl_j}(p) + \sum_{q=1}^{N} a_{qjl_j} v_{ql_j}(p) = 0 \tag{11.8}$$

with

$$a_{qjl_j} = \int_0^\infty \frac{u^2 \mathrm{d}u}{(2\pi)^3} v^*_{ql_j}(u)\tilde{\varphi}_{jl_j}(u). \tag{11.9}$$

We see that a given angular momentum l defines a group of separable potentials. For example, the states $j = 1s, 2s, 3s, \ldots$ enter the group $l = 0$, $j = 2p, 3p, 4p, \ldots$ enter the group $l = 1$, etc. The functions $g_j(\mathbf{p}) = \left(\varepsilon_j - \frac{p^2}{2}\right)\tilde{\varphi}_j(\mathbf{p})$ are called the vertex functions. They define the components of the separable potentials.

We denote $v_n(\mathbf{p}) = v_{nl}(p)Y_{l,m}(\theta_p, \phi_p)$ and redefine in (11.7) $\sum_{q=1}^{N}\sum_{l=0}^{L}\sum_{m=-l}^{l}$ by $\sum_{n=1}$ (do not confuse n with the principal quantum number). Equation (11.7) can be written in matrix form as follows

$$\mathbf{G} + \mathbf{A}\mathbf{V} = 0,$$

or

$$\mathbf{V} = -\mathbf{A}^{-1}\mathbf{G},$$

where the components of $\mathbf{V}$ are the unknown $v_n(\mathbf{p})$. For the matrix $\mathbf{A}$ we obtain a matrix equation from (11.8)

$$\Gamma = \mathbf{A}\mathbf{A}^T, \tag{11.10}$$

where $\mathbf{A}^T$ denotes the transpose matrix of $\mathbf{A}$. The elements of the matrix Γ are known and given by:

$$\Gamma_{ij} = \int \frac{\mathrm{d}^3 u}{(2\pi)^3}\tilde{\varphi}^*_i(\mathbf{u})\left(\frac{1}{2}u^2 - \varepsilon_j\right)\tilde{\varphi}_j(\mathbf{u}).$$

Equation (11.10) can have an infinite number of solutions for the elements of matrix $\mathbf{A}$ within any ℓ-block, if the number of states we take into account in each block is more than one. If we choose matrix $\mathbf{A}$ to be triangular, we obtain a unique solution for the components of the separable potentials. For example, let us consider $\ell = 0$ and write from (11.8)

$$\left(\varepsilon_{1s} - \frac{p^2}{2}\right)\tilde{\varphi}_{1s}(p) + a_{11}v_{1s}(p) = 0,$$

$$\left(\varepsilon_{2s} - \frac{p^2}{2}\right)\tilde{\varphi}_{2s}(p) + a_{21}v_{1s}(p) + a_{22}v_{2s}(p) = 0.$$

This system of linear equations allows to determine components of the separable potential, and the integrals (11.9) allow to determine all unique positive coefficients

a_{11}, a_{21}, a_{22}. We have tested our approach with several cases of symmetric matrix **A**, but have not found any significant difference.

The continuum states for a separable potential follow from the definition of the potential. They are important for the calculation of the ionisation yield and the electron energy spectrum. We get from (11.7)

$$\left(\frac{k^2}{2} - \frac{p^2}{2}\right)\tilde{\varphi}^-(\mathbf{k},\mathbf{p}) + \sum_{n=1}^{N} C_n(\mathbf{k})v_n(\mathbf{p}) = 0, \quad C_n(\mathbf{k}) = \int \frac{\mathrm{d}^3u}{(2\pi)^3} v_n^*(\mathbf{u})\tilde{\varphi}^-(\mathbf{k},\mathbf{u}). \tag{11.11}$$

and

$$\tilde{\varphi}^-(\mathbf{k},\mathbf{p}) = (2\pi)^3\delta(\mathbf{k}-\mathbf{p}) - \frac{2}{k^2 - p^2 - \mathrm{i}0}\sum_{j=1}^{N} C_n(\mathbf{k})v_n(\mathbf{p}) \tag{11.12}$$

For the coefficients $C_n(\mathbf{k})$, we obtain the linear system of algebraic equations

$$C_n(\mathbf{k})[1 + \lambda_{nn}] + \sum_{j\neq n}^{N} \lambda_{nj}C_j(\mathbf{k}) = v_n^*(\mathbf{k}),$$

with

$$\lambda_{nj} = 2\int \frac{\mathrm{d}^3u}{(2\pi)^3}\frac{v_n^*(\mathbf{u})v_j(\mathbf{u})}{k^2 - p^2 - \mathrm{i}0}.$$

For atomic hydrogen all the integrals can be evaluated analytically.

11.2.3 TDSE with Separable Potentials

Let us go back to the TDSE (11.4) in the momentum space and define the action

$$S(\mathbf{p},t) = \frac{1}{2}\int_0^t \left(\mathbf{p} + \frac{1}{c}A(\xi)\mathbf{e}\right)^2 \mathrm{d}\xi.$$

We also define the functions

$$F_n(t) = \int \frac{\mathrm{d}^3u}{(2\pi)^3} v_n^*(\mathbf{u})\tilde{\Phi}_V(\mathbf{u},t), \tag{11.13}$$

and write the solution of (11.4) as

$$\tilde{\Phi}_V(\mathbf{p},t) = e^{-\mathrm{i}S(\mathbf{p},t)}\left[\tilde{\varphi}_0(p) + \mathrm{i}\sum_{n=1}^{N} v_n(\mathbf{p}) \int_0^t \mathrm{d}\xi\, F_n(\xi) e^{\mathrm{i}S(\mathbf{p},\xi)}\right]. \tag{11.14}$$

By inserting (11.14) into (11.13), we obtain a system of coupled Volterra equations for the functions $F_n(t)$. We can write this system in matrix form as follows

$$\mathbf{F}(t) = \mathbf{F}_0(t) + \int_0^t \mathbf{K}(t,\xi)\mathbf{F}(\xi)\mathrm{d}\xi.$$

The analytical expressions for the free term $\mathbf{F}_0(t)$ and the kernel $\mathbf{K}(t,\xi)$ can be found in [8].

Let us discuss (11.14). If we turn off the external field, then, from (11.4), we obtain

$$\tilde{\Phi}_V(\mathbf{p},t) = \tilde{\varphi}_0(p)e^{-\mathrm{i}\varepsilon_0 t}. \tag{11.15}$$

It is thanks to the integral term in (11.14) that $\tilde{\Phi}_V(\mathbf{p},t)$ tends to the hydrogen ground state when the field is zero. It means that we cannot take the term $e^{-\mathrm{i}S(\mathbf{p},t)}\tilde{\varphi}_0(p)$ as a zero order approximation and build an iterative series out of it. Indeed, this free wavepacket in (11.14) disperses in the configuration space even in the absence of the field, which contradicts the meaning of a stationary state. This observation is discussed further in the context of SFA in [22].

If the separable potentials have been generated by imposing that they support N bound states, the ionisation yield $P(t)$ can be calculated as

$$P(t) = 1 - \sum_{n=1}^{N} |\langle\tilde{\varphi}_n|\tilde{\Phi}(t)\rangle|^2. \tag{11.16}$$

11.2.4 Gauge Invariance and Separable Potentials

We have noted above that the TDSE with non-local separable potentials is not gauge invariant. If we put $\tilde{\Phi}_V(\mathbf{p},t) = \tilde{\Phi}_L(\mathbf{p} + \frac{1}{c}A(t)\mathbf{e},t)$ into (11.4), which we reproduce here for clarity

$$\left[\mathrm{i}\frac{\partial}{\partial t} - \frac{1}{2}(\mathbf{p} + \frac{1}{c}A(t)\mathbf{e})^2\right]\tilde{\Phi}_V(\mathbf{p},t) + \sum_{n=1} v_n(\mathbf{p}) \int \frac{\mathrm{d}^3u}{(2\pi)^3} v_n^*(\mathbf{u})\tilde{\Phi}_V(\mathbf{u},t) = 0, \tag{11.17}$$

we get

$$\left[\mathrm{i}\frac{\partial}{\partial t}-\frac{1}{2}p^2-\mathrm{i}E(t)(\mathbf{e}\cdot\boldsymbol{\nabla}_p)\right]\tilde{\Phi}_L(\mathbf{p},t)+\sum_{n=1}v_n(\mathbf{p}-\frac{1}{c}A(t)\mathbf{e})\times \int\frac{\mathrm{d}^3u}{(2\pi)^3}v_n^*(\mathbf{u}-\frac{1}{c}A(t)\mathbf{e})\tilde{\Phi}_L(\mathbf{u},t)=0. \tag{11.18}$$

There are two equivalent ways to obtain (11.18) from (11.5):

$$\frac{4\pi Z}{|\mathbf{p}-\mathbf{u}|^2}\to\sum_{n=1}v_n(\mathbf{p})v_n^*(\mathbf{u}),$$

or

$$\frac{4\pi Z}{|\mathbf{p}-\mathbf{u}|^2}\to\sum_{n=1}v_n(\mathbf{p}-\frac{1}{c}A(t)\mathbf{e})v_n^*(\mathbf{u}-\frac{1}{c}A(t)\mathbf{e}).$$

A question arises: how to generate the time dependent separable potential components v_n in terms of the (time independent) bound state wave functions? To answer this question, we consider the following TDSE

$$\left[\mathrm{i}\frac{\partial}{\partial t}-\frac{1}{2}(\mathbf{p}-\frac{1}{c}A(t)\mathbf{e})^2-\mathrm{i}E(t)(\mathbf{e}\cdot\boldsymbol{\nabla}_p)\right]\tilde{\varphi}_{jL}(\mathbf{p},t)+\int\frac{\mathrm{d}^3u}{(2\pi)^3}\frac{4\pi Z}{|\mathbf{p}-\mathbf{u}|^2}\tilde{\varphi}_{jL}(\mathbf{u},t)=0. \tag{11.19}$$

This equation has the same Coulomb spectrum when the external field is zero. It means that in the configuration space, the solution $\tilde{\varphi}_{jL}(\mathbf{r},t)$ is a Coulomb function, multiplied by the phase factor, present in Göppert-Mayer transformation (11.3), while in momentum space we have

$$\tilde{\varphi}_{jL}(\mathbf{p},t)=\tilde{\varphi}_{jV}(\mathbf{p}-\frac{1}{c}A(t)\mathbf{e})e^{-\mathrm{i}\varepsilon_j t}. \tag{11.20}$$

To the best of our knowledge, the first one who noticed that was Faisal in [26]. With time dependent separable potentials (11.19) writes

$$\left[\mathrm{i}\frac{\partial}{\partial t}-\frac{1}{2}(\mathbf{p}-\frac{1}{c}A(t)\mathbf{e})^2-\mathrm{i}E(t)(\mathbf{e}\cdot\boldsymbol{\nabla}_p)\right]\tilde{\varphi}_{jL}(\mathbf{p},t)+ \sum_{n=1}v_n(\mathbf{p}-\frac{1}{c}A(t)\mathbf{e})\int\frac{\mathrm{d}^3u}{(2\pi)^3}v_n^*(\mathbf{u}-\frac{1}{c}A(t)\mathbf{e})\tilde{\varphi}_{jL}(\mathbf{u},t)=0. \tag{11.21}$$

By substituting $\tilde{\varphi}_{jL}(\mathbf{u}, t)$ by its expression (11.20) we obtain, after changing variables (compare with (11.7))

$$\left[\varepsilon_j - \frac{1}{2}p^2\right]\tilde{\varphi}_{jV}(\mathbf{p}, t) + \sum_{n=1} v_n(\mathbf{p}) \int \frac{\mathrm{d}^3 u}{(2\pi)^3} v_n^*(\mathbf{u})\tilde{\varphi}_{jV}(\mathbf{u}, t) = 0. \tag{11.22}$$

Thus, if one has the TDSE (11.17) in the V-gauge, using the time-independent separable potentials, then (11.18) is its gauge partner, but with time dependent separable potentials. It is a family of gauge invariant solutions.

Equation (11.18) can be written down, however, with time independent separable potentials, defined by the same spectral functions. Equation (11.17) will be defined by time-dependent components with $\mathbf{p} + \frac{1}{c}A(t)\mathbf{e}$ as an argument. We will have another family of gauge invariant solutions as the operators in brackets of (11.17) and (11.18) differ. This is a price to pay for using separable potentials.

11.2.5 Results

From the numerical point of view, the calculations both for atoms and molecules are inexpensive. It can be seen from the form of the $F_n(t)$ function in (11.13) that the spatial dependence is treated analytically. The set of Volterra integral equations of second kind in time for F functions are solved using a block-by-block method (a grid in time), using the GPUs to evaluate the kernels $K(t, \xi)$ for different time points before propagation.

In Figs. 11.1 and 11.2 we compare the predictions of the SPAM model with the experiment for a low frequency pulse, and with TDSE calculations for a high frequency pulse correspondingly (more results are given in [5–8]). For reference, the potential in the case 1s and 2p states included is given by

$$\frac{4\pi}{|\mathbf{p} - \mathbf{u}|^2} \approx \frac{16\pi}{(p^2 + 1)(u^2 + 1)} + \frac{32\pi^2}{3} \frac{(\mathbf{p} \cdot \mathbf{u})}{(p^2 + 1/4)^2(u^2 + 1/4)^2}$$

In the experiment, presented in [15], the authors consider a hydrogen atom, interacting with a laser pulse of frequency of 0.0723 a.u. (630 nm wave length), 10 cycles pulse duration and of peak intensity of 6.5×10^{13} W/cm^2. In Fig. 11.1 a comparison of this experimental spectrum with a SPAM model calculation, with 1s and 2p states included, is presented (the experimental spectrum is normalised to the theoretical one). One can notice an agreement for the peak positions for higher electron energies (> 1 a.u.). At lower energies we do not observe a good agreement for two reasons:

- the slow emitted electron is described by a plane wave which neglects the influence of the binding potential;
- the ac-Stark shift is not properly included in our SPAM model since it involves only two levels (1s and 2p).

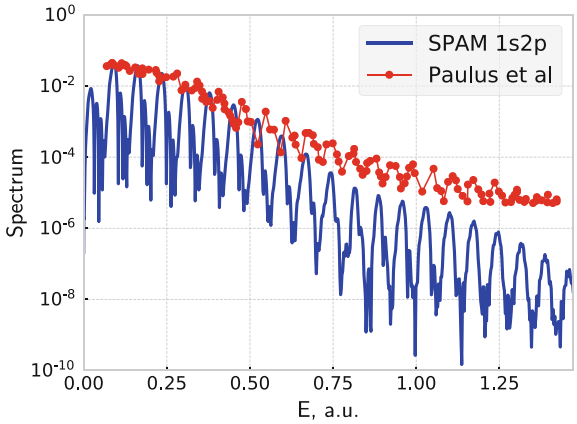

Fig. 11.1 Electron energy spectrum resulting from the interaction of atomic hydrogen with a laser pulse of frequency 0.0723 a.u. (630 nm), 10 cycles duration and with peak intensity 6.5×10^{13} W/cm^2. The red curve is the experimental data from [15], blue curve is the results of calculation with a SPAM model with 1s and 2p states included. Experimental data is normalised to the maximum of the theoretical spectrum. Theoretical vector potential is described by a sine squared envelope

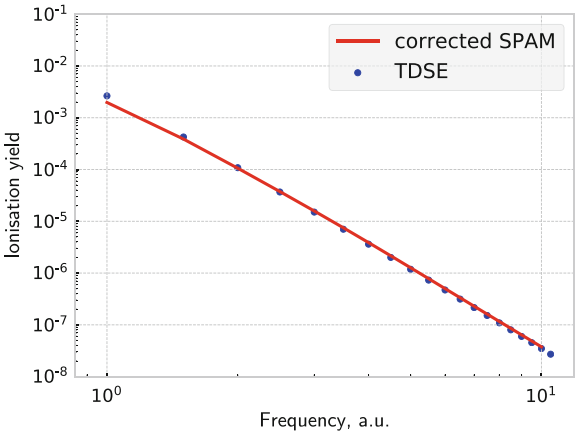

Fig. 11.2 Dependence of the ionisation yield of the H atom on the laser pulse frequency for a sine squared pulse of 2 cycle duration and 10^{14} W/cm^2 peak intensity. The solid line has been obtained by using our SPAM method which includes only 1s state and the dots show the results of the full TDSE calculation. The perturbation theory calculation in the same regime is given in [27]

In Fig. 11.2 the SPAM, containing only 1s state, is compared with the TDSE calculation results. We consider a laser pulse of 2 cycles full duration and 10^{14} W/cm^2 peak intensity. To obtain a better coincidence of the results, we divided the prediction of SPAM by 2 and obtained the so-called corrected SPAM. This correction is due to the lack of interaction in the final state of the system with the laser field, and is obtained analytically for high frequencies in [27].

11.3 Many-Electron Systems

11.3.1 SAE Approximation

The influence of the electron-electron correlations on the dynamics of the processes of excitation and scattering is actively studied in helium atom, hydrogen anion and recently in H_2 molecules [28]. All other atoms and molecules are described with a treatment where electrons are described independently and moving in the mean field of the nuclei and of the all other electrons (see e.g. Hartree-Fock method and, more recently, the multiconfiguration time-dependent Hartree-Fock method [29–31] and the configuration interaction singles method [32, 33]). The best example of such a treatment is the system of non-linear integrodifferential equations of Hartree-Fock.

This system of integrodifferential equations is very often reformulated in terms of one electron local potentials with Coulomb tail. In this case we obtain a TDSE which is particularly attractive to treat single ionisation of a molecule in a pulsed field. This is essentially the SAE approximation, when this "active" electron under the external perturbation, is leaving the atom, and all other electrons are frozen. This approximation is of a particular interest for separable potential application when the separable potentials are built in terms of vertex functions of a single electron. Usually these separable potentials are generated numerically when the one-particle wave function is taken from tables or generated with public codes.

When considering an external electromagnetic field as a perturbation that leads to the emission of an electron from an outer atomic shell, one has to use more complicated separable potentials that account for the excitation of the active electron. It allows one to account for different processes which is more adequate in this case. To find out what can be described with our SPAM model and in which frequency and intensity domains, we consider below a rather complicated process of single ionisation in a laser field, for the hydrogen anion, hydrogen molecule and water molecule.

11.3.2 Hydrogen Anion

A full solution of a TDSE for H^- is feasible at a current level of computer resources. It has two electrons like a helium atom, for which the exact dipole approximation calculations exist since the end of the last century [37–39]. For the hydrogen anion several independent calculations have been made too [35, 39–41].

From the point of view of the applicability of the SPAM model, the hydrogen anion has a major advantage: the anion becomes neutral once one of the electrons is detached, implying that the SPAM model and the short range potential approximation should work beautifully, as the potential does not have a Coulomb tail [42].

The ground state of the anion $1s^2$ is incredibly weakly bound, having binding energy of -0.0277 a.u. only [43].

The experiments on the photodetachment in a strong laser field are quite difficult to carry out, but a few exist [44–48]. The main difficulty is the depletion of negative ions by a low order detachment process at the fore front of the pulse [49, 50]. The intensity there is low, but sufficient for a many photon detachment process. The first observation of such many photon detachment, analogous to above threshold ionisation, was reported in the F^-, Cl^-, Au^- ions [44–47]. Their outer electron binding energy is much higher than the one of H^-, so it was simpler experimentally.

The SPAM model calculations for H^- are very similar to those for atomic hydrogen with only 1s state. However, the ground state wave function, as given by Yamaguchi [51], is slightly different:

$$\tilde{\varphi}(\mathbf{r}) = \frac{\sqrt{2\kappa\beta(\kappa+\beta)}}{\beta-\kappa}\frac{e^{-\kappa r}-e^{-\beta r}}{r}Y_{00}(\theta,\phi), \quad \int \mathrm{d}^3 r\ |\tilde{\varphi}(\mathbf{r})|^2 = 1, \qquad (11.23)$$

with

$$\kappa = 0.235, \quad \varepsilon = -\frac{\kappa^2}{2} = -0.0276, \quad \beta = 0.913.$$

Here κ and β are fitting parameters. On the basis of this wave function we generate the corresponding separable potential in the same way, like we do it for atomic hydrogen (see (11.8) and after).

The comparison of the ionisation yield dependence on the intensity for different calculations is presented in the Fig. 11.3. It has to be mentioned, that the SPAM result in this case is not multiplied by any factor. The prediction of the SPAM model lies quite close to the results obtained by Bachau et al. [34], Scrinzi et al. [35] that take accurately into account the electron-electron correlations.

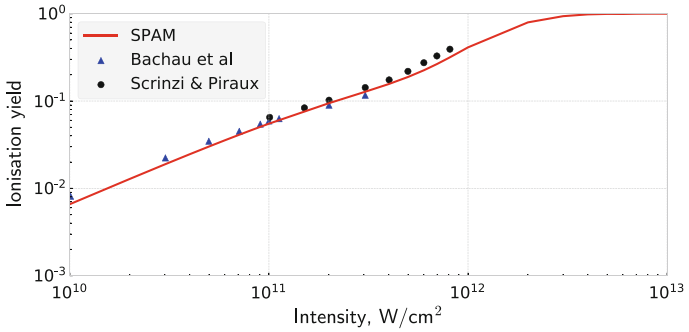

Fig. 11.3 Comparison of the SPAM ionisation yield intensity dependence with more sophisticated calculations from [34, 35] that take electron-electron interaction into account. Hydrogen anion interacts with a sine squared laser pulse of 8 cycles duration and 0.03 a.u. (1520 nm) photon energy. SPAM is presented by a red full line; calculation from [34]—blue triangles; calculation from [35]—black circles

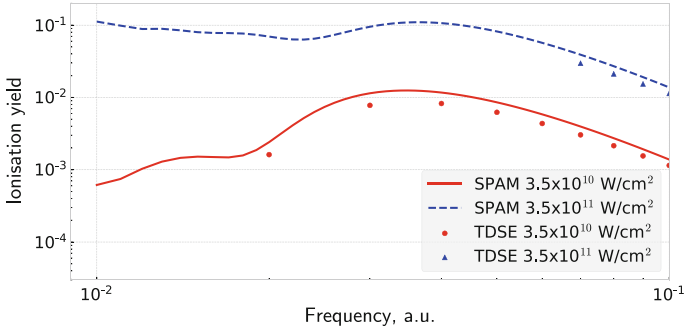

Fig. 11.4 Ionisation yield of H^- versus external field frequency. The duration of the pulse is fixed to 2 cycles, the peak intensity is 3.5×10^{10} W/cm^2 for the full red line (SPAM) and circles (full TDSE [36]) and 3.5×10^{11} W/cm^2 for the dashed blue line (SPAM) and triangles (full TDSE [36])

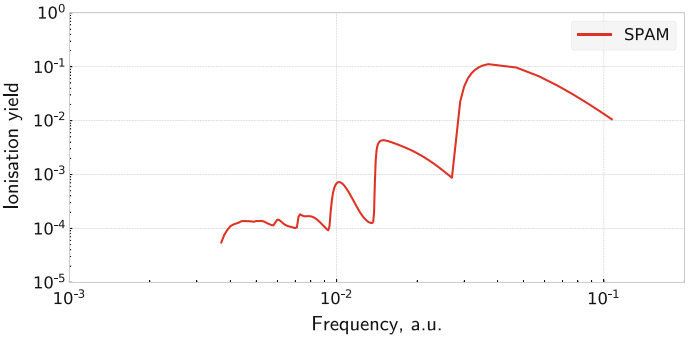

Fig. 11.5 Ionisation yield of the SPAM model of H^- versus external field frequency. The duration of the pulse is fixed to 64 cycles and the peak intensity is 3.5×10^{10} W/cm^2. The cusps result from the closing of different channels

The good agreement of the SPAM prediction with other approaches in the case of the negative ion can be explained by the absence of the Coulomb interaction in the final state. As shown analytically in [8], the difference between the SPAM prediction for atomic hydrogen with respect to the full TDSE calculation is mainly due to the short range of the approximate model potential. In the case of hydrogen anion this approximation is much closer to the real system, leading to a much better agreement.

In Fig. 11.4, we consider the ionisation yield as a function of the frequency for two intensities 3.5×10^{10} W/cm^2 and 3.5×10^{11} W/cm^2 and a total pulse duration of 2 optical cycles. The agreement with the full calculation is slightly worse, although the shape of the curves is the same. The differences are attributed to the fact that the Yamaguchi potential does not describe the electrons on the same footing as it should be.

In Fig. 11.5, the ionisation yield for H^- is plotted versus the external field frequency for a very long pulse of 64 optical cycles full duration. Since the intensity

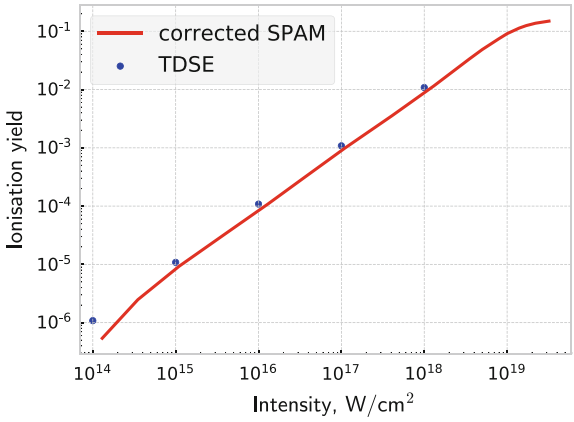

Fig. 11.6 Ionisation yield versus external field intensity for H_2 molecule, interacting with a pulse of 6 cycles full duration and 5 a.u. photon energy. The red solid line is corrected SPAM model prediction and blue dots are TDSE [53]

3.5×10^{10} W/cm^2 is very low and the pulse is very long, the closing of different ionisation channels is clearly visible and manifests itself by the presence of a succession of so-called Wigner cusps.[2]

11.3.3 Hydrogen Molecule

Molecular hydrogen is a very simple diatomic molecule. However, it is only very recently that physicists suceeded to obtain exact numerical results for its evolution in a laser field, taking into account all the electronic and nuclear degrees of freedom [28, 54].

In Figs. 11.6 and 11.7 we compare the predictions for the ionisation yield of the SPAM model (with a correction, discussed in detail in [27]) with the full TDSE calculation [53]. In Fig. 11.6 the laser field frequency is fixed to 5 a.u. and the total pulse duration is 6 optical cycles. The single ionisation probability, as a function of the laser pulse peak intensity shows good agreement, despite the fact that in some cases SAE fails to describe the H_2 molecule [55].

In Fig. 11.7 the laser pulse peak intensity is fixed to 4×10^{14} W/cm^2 and the total pulse duration is 2 optical cycles. Again, the single ionisation probability, as a function of the laser pulse frequency shows relatively good agreement. A strong disagreement for lower frequencies around the ionisation threshold -0.566 a.u. is attributed to the strong influence of the binding potential on the slow electrons, and the important role played by the intermediate states in this region (there are no intermediate states in this SPAM model).

[2]Cusp is an abrupt change of the photodetachment cross section which violates the Wigner's threshold law [52].

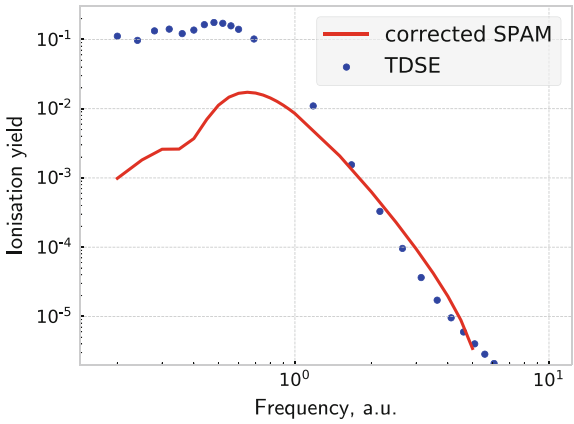

Fig. 11.7 Ionisation yield versus external field frequency for H_2 molecule interacting with a pulse of 2 cycles duration and 4×10^{14} W/cm^2 peak intensity. The red solid line is the corrected SPAM model prediction and blue dots are TDSE [53]

11.3.4 Water Molecule

In this contribution we also consider the $1b_1$ orbital (the HOMO—highest occupied molecular orbital) of water molecule. As the water molecule has 5 occupied orbitals, why do we choose the $1b_1$ orbital?

HOMO $1b_1$ is essentially a 2p atomic orbital of the oxygen atom with very little influence of each hydrogen atom. Ionization of the water HOMO orbital leaves the geometry of the molecule unchanged, thus allowing us to apply the fixed nuclei approximation as the vibrational excitation is low. Farrell et al. showed that by contrast to the ionization of the HOMO, the single ionization of the second least bound orbital $3a_1$ (HOMO-1) triggers a fast nuclear dynamics of the molecular ion and strongly excites the bending mode at photon energies around 0.54 a.u. [57]. In fact, the period of the fastest oscillation in the water molecule, namely the asymmetrical stretching of the OH bonds, is 8.9 fs which is much longer than the pulse durations we consider here. In other words, we can assume that the molecule is frozen during its interaction with the pulse.

To generalize the separable model to the case of the water molecule, we first generate the spatial part $\Phi_0(\mathbf{r})$ of the HOMO $1b_1$ in the configuration space. The molecule lies in the yz plane, with the z axis (and the polarisation vector) passing through the oxygen atom, and the hydrogens are equally distanced from this axis. The spatial part of the molecular orbital is obtained by geometry optimization with the GAMESS(US) program in the Hartree-Fock approximation [58]. Instead of Hartree-Fock one could use DFT, it would not change much, as long as one uses experimental orbital energies instead of the ones generated by GAMESS(US) as they are strongly influenced by the method while the wave functions are not.

The general expression of a molecular orbital α, denoted by $\Phi_\alpha(\mathbf{r})$, is:

$$\Phi_\alpha(\mathbf{r}) = \sum_{j=1}^{3} \sum_{\gamma_j} C_{\gamma_j,\alpha}\, G_{\gamma_j}(\mathbf{r} - \mathbf{R}_j)$$

where index j designates each nucleus in the molecule. The second summation runs over the atomic orbitals around each nucleus and G_{γ_j} is a so-called contracted gaussian from a 6–31G basis set in the present case. $\mathbf{r} - \mathbf{R}_j$ is the electronic coordinate relative to the nucleus j. The coefficients $C_{\gamma_j,\alpha}$ are the ones generated by the GAMESS(US) program.

Since, to the best of our knowledge, there is no experiment performed for a water molecule in a laser field for frequencies above the water molecule ionisation threshold, we compare our results to those obtained with another SAE calculation [56]. They use DFT LB94 exchange-correlation functional with a coulomb tail to generate the Kohn-Sham orbitals that constitute the basis set. The Hamiltonian describes the motion of the active electron in the potential formed by the nuclei and the remaining frozen electrons. In the SAE approximation this leads to the frozen Hartree-Fock, or static-exchange Hamiltonian.

Since the full final momentum wave packet is available in the SPAM model, any information about the system can be easily extracted. The absence of the intermediate states means however that regimes where these states are important, like low frequency ionisation, cannot be treated accurately. Being a SAE approach, one neglects all the dynamical interactions between the particles. Finally, the Born Oppenheimer approximation neglects all the processes related to the motion of the nuclei. Nevertheless, the SPAM model allows one to make predictions for any complex system, where the aforementioned approximations are adequate, in the single photon and ultrashort pulse regimes. The SPAM model is very scalable, so the limits on the size of the system are given by the hardware resources only. All the calculations have been performed in the 6-31G basis set. We are not aware of any significant discrepancies in our calculations that could be attributed to the incompleteness of this basis.

In order to have some idea about how accurate is the prediction of the SPAM model for high frequencies, we ran the SAE-TDSE code from [56] in the 1-photon ionisation regime and compared the ionisation yield prediction of these two SAE models (see Fig. 11.8). Laser pulse total duration was fixed to 2 optical cycles and peak intensity was fixed to 4×10^{14} W/cm^2. A significant difference between these models is the fact that for SAE-TDSE the full Coulomb potential has been taken into account in generating the one-electron orbital basis, thus we suggest to correct the SPAM result with the same factor as for atomic hydrogen. In fact, we have perfect agreement between these models for high frequencies, and poor agreement for the photon energies near the ionisation threshold. This can be explained by the fact that SAE-TDSE uses 6000 Kohn-Sham orbitals to propagate the wave function and thus supports some intermediate configurations, while in SPAM model we don't have any intermediate state at all.

We can see in Fig. 11.9 that the corrected SPAM coincides with SAE-TDSE in a wide intensity range as well. This agreement of the corrected SPAM model and SAE-TDSE approach in a wide intensity and frequency range indicates that the SPAM

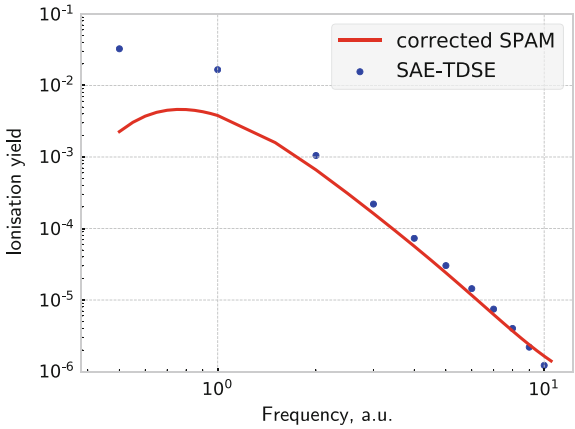

Fig. 11.8 The molecule lies in *yz* plane. Dependence of the ionisation yield of two water molecule models on the photon energy for a sine squared pulse of 2 cycles full duration and 4×10^{14} W/cm^2 peak intensity. The solid line has been obtained by using our corrected SPAM method, the dots show the results of SAE-TDSE calculation [56]

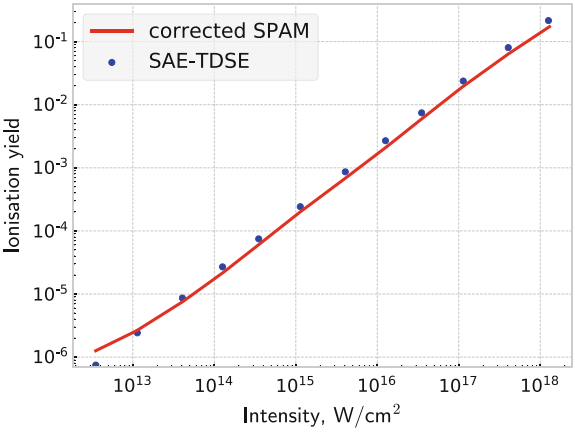

Fig. 11.9 The molecule lies in *yz* plane. Dependence of the ionisation yield of two water molecule models on the laser pulse peak intensity for a sine squared pulse of 6 cycles full duration and 5 a.u. photon energy. The solid line has been obtained by using our corrected SPAM method, the dots show the results of the SAE-TDSE calculation [56]

correction factor does not depend on intensity or on frequency in the high frequency regime.

11.4 Summary and Conclusions

We have developed the SPAM model in the case of the interaction of atomic hydrogen with a laser pulse. In particular, we have analysed in depth the domain of validity of this model and calculated electron energy spectra which have been compared to the experimental one and to those obtained by solving the TDSE numerically.

Furthermore, we have extended SPAM method to the treatment, within the SAE approximation, of the interaction of a complex quantum systems with high frequency ultrashort laser pulses.

As a first application we have considered the photodetachment of H^- which is a quantum system that is particularly well adapted to our SPAM approach. We obtain in this case a very good agreement with full TDSE results.

The SPAM model has also been applied to the case of the single ionisation of the HOMO orbital of the hydrogen and water molecules by a high frequency ultrashort laser pulse. Our results for the ionisation yield clearly show the pertinence of the SPAM method in its application to more complex systems.

Acknowledgements We are grateful to Professor A. Saenz and his group for running their code for molecular hydrogen for us to be able to compare our results with theirs. A. G. is "aspirant au Fonds de la Recherche Scientifique (F. R. S.-FNRS)". Yu.P. thanks the Université catholique de Louvain (UCL) for financially supporting several stays at the Institute of Condensed Matter and Nanosciences of the UCL. F. M. F. and P. F. O'M. gratefully acknowledge the European network COST (Cooperation in Science and Technology) through the Action CM1204 "XUV/X-ray light and fast ions for ultrafast chemistry" (XLIC) for financing several short term scientific missions at UCL. P.D. and A.G. acknowledge COST XLIC and F. R.S-FNRS for financing two short term scientific missions (STSM) in Trieste, Italy, and participation in COST XLIC meetings. The present research benefited from computational resources made available on the Tier-1 supercomputer of the Federation Wallonie-Bruxelles funded by the Region Wallonne under the Grant No. 1117545 as well as on the supercomputer Lomonosov from Moscow State University and on the supercomputing facilities of the UCL and the Consortium des Equipements de Calcul Intensif (CECI) en Federation Wallonie-Bruxelles funded by the F.R.S.-FNRS under the convention 2.5020.11. Y.P. is grateful to the Russian Foundation for Basic Research (RFBR) for financial support under the grant No. 16-02-00049-a. O.Ch. acknowledges support from the Hulubei-Meshcheryakov program JINR-Romania.

References

1. E.W. Schmid, H. Zieǵelmann, *The Quantum Mechanical Three- Body Problem: Vieweg Tracts in Pure and Applied Physics*, vol. 2 (Elsevier, 2017)
2. N. Zh. Takibayev, Class of model problems in three-body quantum mechanics that admit exact solutions, Phys. At. Nucl. **71**(3), 460–468 (2008)
3. N. Zh. Takibaev, Solution of electron equation for the ion system H_2^+ (in Russian). Izv. Nats. Akad. Nauk, Ser. Fiz. Mat. **2**, 80–85 (2008)
4. S. Giraud et al., Strong field atomic ionization dynamics: role of the Coulomb potential studied by means of a model. Proc. SPIE **6165**, 61650D (2006)
5. H. M. Tetchou Nganso et al. On the role of the Coulomb potential in strong field atomic ionization dynamics. J. Electron Spectrosc. Relat. Phenom. **161**(1–3), 178–181 (2007), https://doi.org/10.1016/j.elspec.2006.10.006
6. H.M. Tetchou Nganso et al. Ionization of atoms by strong infrared fields: solution of the time-dependent Schrödinger equation in momentum space for a model based on separable potentials. Phys. Rev. A **83**(1), 013401 (2011)
7. H.M. Tetchou Nganso et al., Interaction of a model atom exposed to strong laser pulses: role of the Coulomb potential. Phys. Rev. A **87**(1), 013420 (2013)
8. A. Galstyan et al., Modelling laser-atom interactions in the strong field regime. Eur. Phys. J. D **71**(4), 97 (2017)
9. H. Rottke, K.H. Welge, Photoionization of the hydrogen atom near the ionization limit in strong electric fields. Phys. Rev. A **33**(1), 301–311 (1986)
10. H. Rottke et al., Multiphoton ionization of atomic hydrogen in intense subpicosecond laser pulses. Phys. Rev. Lett. **64**(4), 404–407 (1990)

11. M. Dörr et al., The energy spectrum of photoelectrons produced by multiphoton ionization of atomic hydrogen. J. Phys.B Atomic Mol. Opt. Phys. **25**(12), L275–L280 (1992)
12. Y. Gontier et al., Five-photon ionization of atomic hydrogen at wavelengths around the threshold for four-photon ionization. Phys. Rev. A **46**(9), 5594–5599 (1992)
13. H. Rottke et al., Atomic hydrogen in intense short laser pulses: a new series of photoelectron peaks from above-threshold ionization. J. Phys. B: Atomic, Mol. Opt. Phys. **26**(2), L15–L22 (1993)
14. H. Rottke et al., Atomic hydrogen in a strong optical radiation field. Phys. Rev. A **49**(6), 4837–4851 (1994)
15. G.G. Paulus et al., High-order above-threshold ionization of atomic hydrogen using intense, ultrashort laser pulses. J. Phys. B At. Mol. Opt. Phys. **29**(7), L249–L256 (1996)
16. M.G. Pullen et al., Experimental ionization of atomic hydrogen with fewcycle pulses. Opt. Lett. **36**(18), 3660–3662 (2011). https://doi.org/10.1364/OL.36.003660
17. E. Huens et al., Numerical studies of the dynamics of multiphoton processes with arbitrary field polarization: methodological considerations. Phys. Rev. A **55**(3), 2132–2143 (1997)
18. B. Piraux et al., Excitation of Rydberg wave packets in the tunneling regime. Phys. Rev. A **96**(4), 043403 (2017)
19. T.C. Rensink et al., Model for atomic dielectric response in strong, timedependent laser fields. Phys. Rev. A **89**(3), 033418 (2014)
20. T.C. Rensink, T.M. Antonsen, Strong-field ionization and gauge dependence of nonlocal potentials. Phys. Rev. A **94**(6), 063407 (2016), https://doi.org/10.1103/PhysRevA.94.063407
21. S.V. Popruzhenko, Keldysh theory of strong field ionization: history, applications, difficulties and perspectives.J. Phys. B Atomic, Mol. Opt. Phys. **47**(20), 204001 (2014)
22. A. Galstyan et al., Reformulation of the strong-field approximation for lightmatter interactions. Phys. Rev. A **93**(2), 023422 (2016), https://doi.org/10.1103/PhysRevA.93.023422
23. Yu. Popov et al., Strong field approximation within a Faddeev-like formalism for laser-matter interactions. Eur. Phys. J. D **71**(4), 93 (2017), https://doi.org/10.1140/epjd/e2017-70708-7
24. R. Szmytkowski, Alternative approach to the solution of the momentum-space Schroedinger equation for bound states of the N-dimensional problem. Ann. Phys. **524**(6–7), 345–352 (2012)
25. H.S. Cohl, On a generalization of the generating function for Gegenbauer polynomials. Integral Transforms Spec. Funct. **24**(10), 807–816 (2013), https://doi.org/10.1080/10652469.2012.761613
26. F.H.M. Faisal, Gauge-equivalent intense-field approximations in velocity and length gauges to all orders. Phys. Rev. A **75**(6), 063412 (2007)
27. A. Galstyan et al. Ionisation of H2O by a strong ultrashort XUV pulse: a model within the single active electron approximation. Chem. Phys. **504**, 22–30 (2018), https://doi.org/10.1016/j.chemphys.2018.02.014
28. A. Palacios, H. Bachau, F. Martin, Excitation and ionization of molecular hydrogen by ultrashort vuv laser pulses. Phys. Rev. A **75**(1), 013408 (2007)
29. J. Zanghellini et al., An MCTDHF approach to multielectron dynamics in laser fields. Laser Phys. **13**(8), 1064–1068 (2003)
30. T. Kato, H. Kono, Time-dependent multiconfiguration theory for electronic dynamics of molecules in an intense laser field. Chem. Phys. Lett. **392**(4–6), 533–540 (2004)
31. K.L. Ishikawa, T. Sato, A review on ab initio approaches for multielectron dynamics. IEEE J. Sel. Top. Quantum Electron **21**(5), 1–16 (2015)
32. N. Rohringer, A. Gordon, R. Santra, Configuration-interactionbased time-dependent orbital approach for ab initio treatment of electronic dynamics in a strong optical laser field. Phys. Rev. A **74**(4), 043420 (2006)
33. S. Pabst, R. Santra, Strong-field many-body physics and the giant enhancement in the high-harmonic spectrum of xenon. Phys. Rev. Lett. **111**(23) 233005 (2013)
34. H. Bachau et al., Applications of B-splines in atomic and molecular physics. Rep. Prog. Phys. **64**(12), 1815–1944 (2001)
35. Armin Scrinzi and Bernard Piraux, Two-electron atoms in short intense laser pulses. Phys. Rev. A **58**(2), 1310–1321 (1998)

36. G. Lagmago Kamta et al., Ionization of H^- by a strong ultrashort laser pulse. J. Phys. B Atomic Mol. Opt. Phys. **34**(5), 857–868 (2001)
37. J. Purvis et al., Multiphoton ionization of H^- and He in intense laser fields. Phys. Rev. Lett. **71**(24), 3943–3946 (1993)
38. E.S. Smyth, J.S. Parker, K.T. Taylor, Numerical integration of the time-dependent Schrödinger equation for laser-driven helium. Comput. Phys. Commun. **114**(1–3), 1–14 (1998), https://doi.org/10.1016/S0010-4655(98)00083-6
39. E. Foumouo et al., Theory of multiphoton single and double ionization of two-electron atomic systems driven by short-wavelength electric fields: an ab initio treatment Phys. Rev. A **74**(6), 063409 (2006)
40. L.A.A. Nikolopoulos, P. Lambropoulos, Time-Dependent Nonperturbative Theory of H^- in a Strong Laser Field. Phys. Rev. Lett. **82**(19), 3771–3774 (1999)
41. H.-C. Shao, F. Robicheaux , Photodetachment of H^- from intense, short, high-frequency pulses. Phys. Rev. A **93**(5), 053414 (2016)
42. G.W.F. Drake, Second bound state for the hydrogen negative ion. Phys. Rev. Lett. **24**(4), 126–127 (1970)
43. M.A. Kornberg, Multiphoton ionization of H^- at 160 nm: a study on the production of protons. Europhys. Lett. **52**(2), 130–136 (2000)
44. C. Blondel et al., Excess-photon absorption in a negative ion. J. Phys. B: At. Mol. Opt. Phys. **24**(16), 3575–3588 (1991)
45. M.D. Davidson, H.G. Muller, H.B. van Linden, van den Heuvell, Experimental observation of excess-photon detachment of negative ions. Phys. Rev. Lett. **67**(13), 1712–1715 (1991)
46. M.D. Davidson et al., Longer wavelengths require lower intensity in multiphoton detachment of negative ions. Phys. Rev. Lett. **69**(24), 3459–3462 (1992)
47. H. Stapelfeldt et al., Excess-photon detachment in the negative gold ion. Phys. Rev. Lett. **67**(13), 1731–1734 (1991)
48. C.R. Quick et al., Photodetachment of the H- ion. Nucl. Instrum. Methods Phys. Res. Sect. B Beam Interact. Mater. Atoms **56** 205–210 (1991), https://doi.org/10.1016/0168-583X(91)96007-8
49. R. Reichle, H. Helm, I.Y. Kiyan, Photodetachment of H^- in a strong infrared laser field. Phys. Rev. Lett. **87**(24), 243001 (2001)
50. R. Reichle, H. Helm, I.Y. Kiyan, Detailed comparison of theory and experiment of strong-field photodetachment of the negative hydrogen ion. Phys. Rev. A **68**(6), 063404 (2003)
51. Y. Yamaguchi, Two-nucleon problem when the potential is nonlocal but separable I. Phys. Rev. **95**(6), 1628–1634 (1954)
52. J. Slater et al., Alkali negative ions. III. Multichannel photodetachment study of Cs^- and K^-. Phys. Rev. A **17**(1), 201–213 (1978)
53. A. Saenz and his group. *Private Communication*, (2017)
54. Y. Vanne, A. Saenz, Numerical treatment of diatomic two electron molecules using a B-spline based CI method. J. Phys. B: At. Mol. Opt. Phys. **37**(20), 4101–4118 (2004)
55. M. Awasthi, A. Saenz, Breakdown of the single-activeelectron approximation for one-photon ionization of the B1Su + state of H2 exposed to intense laser fields. Phys. Rev A. **81**(6), 063406 (2010)
56. S. Petretti et al., Water molecules in ultrashort intense laser fields. Chem. Phys. **414**, 45–52 (2013), https://doi.org/10.1016/j.chemphys.2012.01.011
57. J.P. Farrell et al., Strong field ionization to multiple electronic states in water. Phys. Rev. Lett. **107**(8), 083001 (2011)
58. M.W. Schmidt et al., General atomic and molecular electronic structure system. J. Comput. Chem. **14**(11), 1347–1363 (1993), https://doi.org/10.1002/jcc.540141112